Numerical Modeling of Experimentally Fabricated InAs/GaAs Quantum Rings

I. Filikhin*, E. Deyneka**, and B. Vlahovic*

*Physics Department, North Carolina Central University, 1801 Fayetteville St.
Durham, NC 27707, USA, branko@jlab.org;
**Center for Advanced Materials and Smart Structures, North Carolina A&T State University,
Greensboro, NC 27411, USA

ABSTRACT

Single subband model for InAs/GaAs quantum rings (QR), with the electron effective mass depending on the confinement energy by the Kane formula is applied for numerical simulation of the capacitance-voltage (CV) spectroscopy experiments. Geometrical parameters chosen for the model are based on the fabrication process for InAs/GaAs QD/QR. The 3D confined energy problem is solved numerically by the finite element method. Obtained results for QR single energy levels are in a good agreement with the CV measurements. Evaluated magnitude of the electron effective mass is also correlates with the FIR spectroscopy data. These results are compared with the existing 2D model calculations. Theoretical estimates for the addition to the ground state energy of QR in the external magnetic field are given, and compared with experimental CV data.

Keywords: quantum rings, electron levels, single tunneled electron

1 INTRODUCTION

Successful fabrication of nano-sized self-assembled quantum dots (QD) and quantum rings (QR) with controlled geometrical properties has highlighted their potential for practical photonic device applications. Well-established process of QD formation by the epitaxial grows and its consecutive transformation into the QR [1, 2] allows producing of 3D structures with the lateral size about 40-60 nm, and the height of 2-8 nm. It is now possible to directly observe discreet energy spectra of QD and QR by the capacitance-voltage (CV) and far infrared (FIR) spectroscopy [1-3]. Related theoretical studies, however, applied either the 2D models, or 3D models that were not reflecting the actual QR fabrication sizes and experimental conditions, therefore had some limitations interpreting the experiments [2-6]. In the presented work a single subband model for InAs/GaAs QD (QR) is applied, where the electron effective mass depends on the confinement energy by the Kane formula [7]. The geometrical parameters of the model are based on the fabrication process for InAs/GaAs QD/QR, for which the experimental CV and FIR data is available [1-3]. We assume that the QD to QR transformation occurs without essential diffusion of GaAs substrate material into the InAs quantum ring. For geometry configuration of the QR a model suggested by Blossey and Lorke [8] was employed. The 3D confined energy problem [9-10] is solved numerically by the finite element method using iterative procedure. Experimental single electron spectra taken from the CV measurements [2, 3] were applied in order to define the additional QR potential, effectively simulating a total contribution of the band-gap deformation potential, the strain induced potential, and the piezoelectric potential [6]. The magnitude of the electron effective mass is compared with the FIR spectroscopy data [3]. These results are accompanied by analysis of the related 2D model calculations [2-3]. Theoretical estimates for the addition to the ground state energy of QR in the external magnetic field are presented, and compared with experimental CV data.

2 MODEL DECRIPTION

The InAs QRs are considered. Quantum rings having a rotational symmetry are embedded into the GaAs substrate. Geometrical parameters of the QR are the height H, the radial width ΔR, and the inner radius R_1 (the outer radius is $R_2 = R_1 + \Delta R$). A cross section of the quantum ring is shown in Figure 1. The following geometrical parameters reported for experimental fabricated QR [1, 2, 11] were used in the model: R_1=10 nm, $R_2 \cong 40$ nm, H=1.5 nm. The previously reported geometry for QD was defined with R_1 = 10 nm, $H \cong 7$ nm [1, 2].

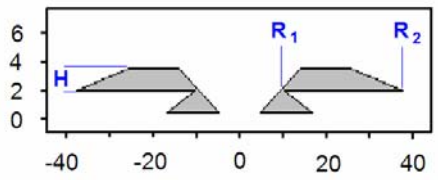

Figure 1: Cross section of the quantum ring.

The volume of the quantum ring is slightly larger then the volume of the initial quantum dot. We attribute this difference to insufficient diffusion of the GaAs substrate material into the InAs quantum ring. Presented QR geometry is analogous to the model suggested in [8].

The 3D heterostructure described above is modeled utilizing the ***kp***-perturbation single subband approach with the energy-dependent quasi-particle effective mass [9-10, 12]. The energies and the wave functions of the single electron in a semiconductor structure are the solutions of the nonlinear Schrödinger equation:

$$\left(-\frac{\hbar^2}{2m^*(x,y,z,E)}\nabla^2 + V(x,y,z) - E\right)\psi = 0, \quad (1)$$

where $V(x,y,z)$ is the band gap potential, proportional to the energy misalignment of the conduction band edges of InAs QR and GaAs substrate. The electron effective mass $m^* = m^*(x,y,z,E)$ is defined by the Kane formula [7] for each area of the QR/Substrate:

$$\frac{m_0}{m^*} = \frac{2m_0P^2}{3\hbar^2}\left(\frac{2}{E_g+E} + \frac{1}{E_g+\Delta+E}\right). \quad (2)$$

Here m_0 is free electron mass, P is Kane's momentum matrix element, E_g is the band gap, and Δ is the spin-orbit splitting of the valence band. E is the ground state confinement energy. $V(x,y,z) = E_0$ inside the substrate, and $V(x,y,z) = 0$ inside the QR. The magnitude of E_0 was calculated as $E_0 = 0.7\left(E_{g,2} - E_{g,1}\right)$. The periodic boundary conditions for the wave function Ψ on the surface side of the QR array unit cell (Fig.1) are chosen to satisfy the relation E_0: $(\vec{k},\vec{\nabla}\Psi) = 0$, where $\vec{k}$ is normal to the surface. The following experimental values [13] were used for the QR (index 1) and the substrate (index 2) components: $(2m_0P_1^2)/\hbar^2$=20.5, $(2m_0P_2^2)/\hbar^2$=24.6, $E_{g,1}$=0.42 eV, $E_{g,2}$=1.52 eV, Δ_1=0.34 eV, Δ_2=0.49 eV, E_0=0.77 eV. Bulk effective masses of InAs and GaAs are $m^*_{0,1}$=0.024 m_0 and $m^*_{0,2}$=0.067 m_0, respectively. The non-linear Schrödinger equation (1) is solved by the iterative procedure, where the solution of the linear Schrödinger equation for each step is numerically obtained by the finite element method (FEM). Details of the numerical treatment were described earlier in [9, 10]. Taking a rotational symmetry of the problem into account, the Eq. (1) can be rewritten in cylindrical coordinates. In this case the energy states are defined by a pair of the quantum numbers (n,l), where n and l are the radial and the orbital quantum numbers, respectively.

3 MODEL WITH THE EFFECTIVE POTENTIAL

That earlier model of QR, which considered only the band-gap potential, could not adequately explain the experimentally observed change in the QR electron effective mass from a bulk value of 0.024 m_0 to the value of 0.063 m_0 [3]. More sophisticated 3D models, with the band-gap deformation potential, the strain-induced potential, and the piezoelectric potential taken into account in addition to the band-gap potential, were recently proposed in [6]. However, a direct comparison of the results [6] and experimental data is not possible because the geometry of QR used in [6] was far from realistic. In order to improve our prior model [10, 12], we have introduced the potential V_s, which simulates an integral effect of all QR potentials listed above, while leaving the realistic geometric parameters intact. The effective potential V_s ~ 0.5 eV has attractive character and acts inside the volume of the quantum ring. Feasibility of the corrected model can be tested by comparing the results of our calculations with the exact solution derived in [6], as shown in Fig. 2. A cross section of the QR used in our model is depicted in Fig. 2a), and the energies of a few low-lying electronic levels are shown in Fig.2b. One can see that there is a good correlation between the two calculations. The observed small mismatch in values of the energy levels can be attributed to a slight difference between cross sections of the quantum rings used by both models.

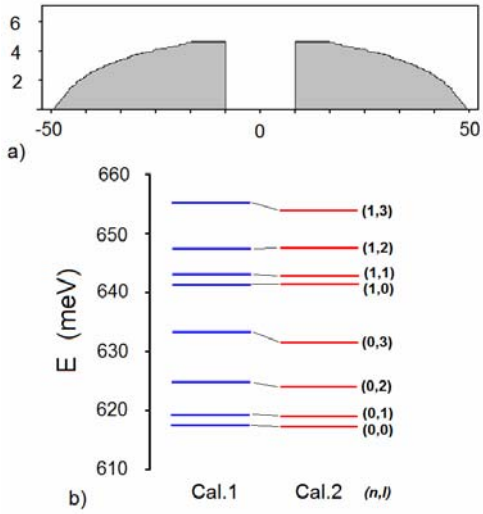

Figure 2 a) Cross section of the quantum ring. b) Energies of the lower levels of a single electron spectrum. The *Cal.1* and *Cal.2* relate to the results of our calculations and the ones of [6], respectively. The quantum numbers (n,l) of the electron states are shown.

4 NUMERICAL RESULTS

The effective potential V_s = 0.55 eV was selected for the interpretation of CV experiments. With this correction the

electron spectra calculation results in localization of the *s*-shell electron level in respect to the bottom conduction band of the GaAs substrate, similar to that, which can be derived from the CV measurements [2]. The s-level energies and the electron effective masses, calculated with (solid circle) and without (open circle) taking the effective potential V_s into account, are shown in Fig. 3. The experimental values for QD and QR are shown as squares for illustration. One can see that the electron effective mass change during the QD to QR transformation is well-reproduced by the Kane's formula.

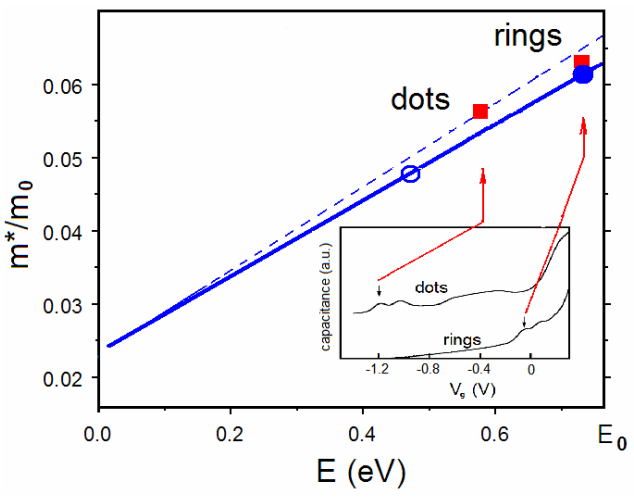

Figure 3. Calculated (circles) and experimentally obtained [1-3] (squares) values for the electron effective mass and *s*-level energy. Solid line is derived by the Kane formula. Dashed line connects bulk values of the effective mass. The insert: the capacitance-gate-voltage traces [2]. First *s*-levels of QD and QR are shown by arrows. The gate-voltage localization of the *s*-levels in respect to the bottom of the GaAs conduction band is mapped onto the energy scale.

The correlation between the *s*-levels of experimental CV data [1] and calculated *s*-levels is shown in Fig. 3 (Insert). Each peak of the capacitance-gate-voltage traces corresponds to the tunneling of a single electron into the quantum ring (quantum dot). The first peak refers to the occupation of the first s-level. For the quantum dot there are two *s* and *p*-shells of the electron levels below the bottom of GaAs conduction band [1-3]. The first level of the d-shell is located above this threshold, and is not observed. Nevertheless, in a weak magnetic field the d-level appears in the spectrum due to the orbital Zeeman effect [1, 4]. Therefore we can define the energy of the *s*-level in respect to the bottom of GaAs conduction band. Recalculation of the gate-voltage to energy can be done by the voltage-to-energy conversion coefficient $f = (e\Delta V)/\Delta E$ which is equal to 7 [1]. For the QR we found that the s-level is located approximately 30~meV below the potential barrier E_0. The excitation energies, calculated at various strengths of the magnetic field B, together with experimental data for a single tunneled electron [3] are shown in Fig. 4. In experiments [2-3] only the resonances with the change in the orbital quantum number $|\Delta l|$=1 are observed. Such resonances were calculated and are shown in Fig. 4, as connected by solid lines. The lines diverging from the point B=0 exhibit the orbital Zeeman splitting for the electron levels with non-zero l with magnetic field increase. The agreement between our results and the experiment is quite satisfactory. The effect of non-parabolicity, taken into account in our model, leads to a significant change in the electron effective mass of QR in respect to the bulk value (according to the relation (2)). For the QR considered above the effective mass of InAs increases from the initial bulk value of $0.024\,m_0$ to $0.0615\,m_0$, which is close to the electron effective mass of $0.063\,m_0$ obtained in FIR experiments [2-3] from the orbital Zeeman splitting.

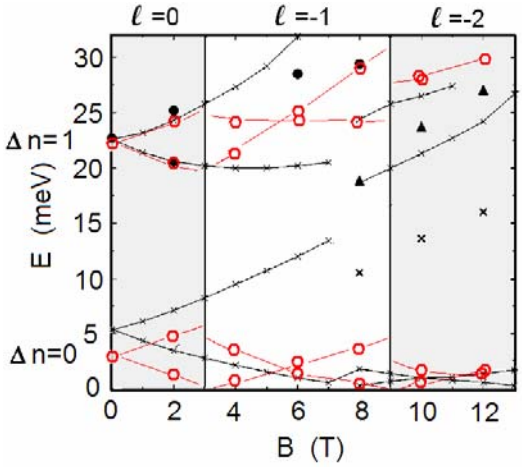

Figure 4. Observed resonance positions [3] of the FIR transmissions at various magnetic field strength *B*. Calculated energies of the excited states are marked by the open squares. Open circles and small crosses are the results of the present work and calculations of [3], respectively. The orbital quantum numbers of ground states are shown.

One can see that our calculations differ from the results obtained by using the planar model [3], particularly, in the magnitude of the period of the electron ground state orbital number transfer in a magnetic field. The calculated first change of l from 0 to -1 occurs at $B \sim$ 3 T, whereas according to [3] it happens at $B \sim$ 7 T. This fact can be understood by considering the relationship between the energy and the magnetic flux Φ for the ideal quantum ring [14] of radius R_0 in a perpendicular magnetic field:

$$E_{(0,l)} = \hbar^2/(2m^* R_0^2)(l + \Phi/\Phi_0)^2, \qquad (3)$$

where $\Phi = \pi R_0^2 B$ is the magnetic flux and $\Phi_0 = h/e$ is the magnetic flux quantum (Φ_0 =4135.7 Tnm^2), e is the electron charge. The relation (3) is approximately holding true in our model as it demonstrated in Table. 1, where the energies of a few first electron levels and the magnitude of the Aharonov-Bohm period [14] obtained from our model and by the model of ideal ring (3) are listed. Note that the Aharonov-Bohm period is defined as the value of magnetic field for the orbital number transfer $|\Delta l|$=1, and is calculated by the expression: $\Delta B = \Phi_0 / (\pi R_0^2)$.

	$\Delta E_{(0,l)}$ meV			ΔB, T
	$l=1$	$l=2$	$l=3$	
3D model	2.8	9.3	17.4	6.0
Ideal ring model	2.5	9.9	22.3	5.3

Table 1: Electron excitation energy $\Delta E_{(0,l)}$ calculated in presented 3D model, and the ideal ring model. The Aharonov-Bohm period ΔB for each model is shown.

For the ideal ring calculation the value of the r-variable at the maximum of the electron wave function $\Psi^2(r,z)r$ is used as the radius of the ring R_0. One can see in Fig. 5 that R_0 is about 16 nm.

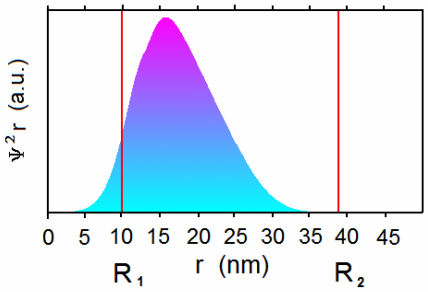

Figure 5. Projection of the electron wave function on the plane normal to the *z*-axis. The locations of the inner R_1 and the outer R_2 radii of the quantum ring are shown.

The value of R_0=14 nm in the model [2, 3] corresponds to a minimum of the parabolic confinement potential. The relation $E_{(0,l)} = \hbar^2/(2m^* R_0^2)(l + \Phi/(2\Phi_0))^2$ is applicable in this case, and can be interpreted as that the model [2, 3] provides the value of $2\Phi_0$ for the magnetic flux quantum.

5 CONCLUSION

InAs/GaAs quantum ring was studied under the energy dependent effective mass approximation. It is found that the incorporation of the effective potential, simulating a total effect of the band-gap deformation potential, the strain induced potential, and the piezoelectric potential into the model of quantum ring allows a qualitative description of experimental data for the single electron. It is shown that the observed deviation of the electron effective mass of QR from its bulk value can be attributed to the non-parabolic effect. The effect of the 3D geometry of QR on the energy of electron levels and the Aharonov-Bohm period was evaluated by comparison with the ideal ring model. We found the ideal ring model can be used for qualitative description of experiment data.

This project is supported by the Department of Defense through grant No. DAAD 19-01-1-0795. I.F. also is partly supported by NASA grant NAG3-804.

REFERENCES

[1] B. T. Miller et al., Phys. Rev. B 56, 7664-6769, 1997.
[2] A. Lorke, R. J. Luyken, A. O. Govorov, and J. P. Kotthaus, J. M. Garcia and P. M. Petroff, Phys. Rev. Lett. 84, 2223-2226, 2000.
[3] A. Emperador, M. Pi, M. Barranko, A. Lorke, Phys. Rev. B. 62, 4573-4577, 2000.
[4] R. J. Warburton, B. T. Miller, C. S. Durr, C. Bodefeld, K. Karrai, Kotthaus, G. Medeiros-Ribeiro, P. M. Petroff, S. Huant, Phys. Rev. B 56, 6764-6773, 1997.
[5] S. S. Li and J. B. Xia, J. Appl. Phys. 89, 3434-3437, 2001.
[6] J. I. Climente, J. Planelles, F. Rajadell, J. Phys.: Condens. Matter 17, 1573-1582, 2005
[7] Kane E. Band Structure of Indium Antimonide. Journal of Physics and Chemistry of Solids, 1, 249-261, 1957.
[8] R. Blossey and A. Lorke, Phys. Rev. E. 65, 021603-021606, 2002.
[9] Y. Li, O. Voskoboynikov, C.P Lee., S.M. Sze, O. Tretyak, J. Appl. Phys. 90, 6416-6420, 2002.
[10] I. Filikhin, E. Deyneka and B. Vlahovic, Modelling Simul. Mater. Sci. Eng. 12, 1121-1130, 2004.
[11] A. O. Govorov, S. E. Ulloa, K. Karrai, R. J. Warburton, Phys. Rev. B 66, 081309(R), 2002.
[12] I. Filikhin, E. Deyneka and B. Vlahovic, Physica E 31, 99–102, 2006.
[13] Handbook Series on Semiconductor Parameters, edited by M. Levinshtein, S. Rumyantsev and M. Shur, (World Scientific, Singapore) 1999.
[14] A. G. Aronov, Yu. V. Sharvin Mod. Phys. 59, 755-755, 1987.